THEORETICAL CALCULATION OF ACOUSTIC-GRAVITY WAVE EXCITATION BY NUCLEAR EXPLOSIONS IN THE ATMOSPHERE

C. A. Newton, et al

Teledyne Geotech

Prepared for:

Air Force Office of Scientific Research

5 March 1973

AL-72-4

.....contributing to man's
understanding of the environment world

THEORETICAL CALCULATION OF ACOUSTIC-GRAVITY WAVE EXCITATION BY NUCLEAR EXPLOSIONS IN THE ATMOSPHERE

BY
C.A. NEWTON, E.A. FLINN and D.G. HARKRIDER

SPONSORED BY
ADVANCED RESEARCH PROJECTS AGENCY

MONITORED BY
AIR FORCE OFFICE OF SCIENTIFIC RESEARCH

ARPA ORDER NO. 1357

5 MARCH 1973

TELEDYNE GEOTECH
ALEXANDRIA LABORATORIES

(Security classification of title, body of abstract and indexing annotation must be entered when the overall report is classified)

1. ORIGINATING ACTIVITY (Corporate author)
Teledyne Geotech
Alexandria, Virginia 22313

2a. REPORT SECURITY CLASSIFICATION
UNCLASSIFIED

2b. GROUP

3. REPORT TITLE
THEORETICAL CALCULATION OF ACOUSTIC-GRAVITY WAVE EXCITATION BY NUCLEAR EXPLOSIONS IN THE ATMOSPHERE

4. DESCRIPTIVE NOTES (Type of report and inclusive dates)
Scientific Interim

5. AUTHOR(S) (First name, middle initial, last name)
C. A. Newton
E. A. Flinn
D. G. Harkrider

6. REPORT DATE
5 Mar 1973

7a. TOTAL NO. OF PAGES
~~33~~ 34

7b. NO. OF REFS
4

8a. CONTRACT OR GRANT NO
F44620-69-C-0082

b. PROJECT NO.
AO 1357

c.
62701D

d.

9a. ORIGINATOR'S REPORT NUMBER(S)
AL-72-4

9b. OTHER REPORT NO(S) (Any other numbers that may be assigned this report)
AFOSR-TR-73-0714

10. DISTRIBUTION STATEMENT
Approved for Public Release; distribution unlimited.

11. SUPPLEMENTARY NOTES
TECH, OTHER

12. SPONSORING MILITARY ACTIVITY
AFOSR(NPP)
1400 Wilson Boulevard
Arlington, Virginia 22209

13. ABSTRACT
From theoretical calculations of acoustic-gravity waves in the period range 40 to 1,000 seconds from various combinations of yield and burst height, we conclude that the power varies as the square of the yield for low-altitude explosions and as the two-thirds power for altitudes above 100 km. For a given yield, the power increases with burst height to a maximum which is found at lower altitudes for higher yields. The affect of variable atmospheric structure along the propagation paths render it possible to make only a rough estimate of yield and no meaningful estimate of burst height. The study also shows that all of the first ten modes are always relatively well excited so that the relative modal structure of a signal is not a good diagnostic for burst height.

DD FORM 1 NOV 68 1473

UNCLASSIFIED
Security Classification

KEY WORDS	LINK A		LINK B		LINK C	
	ROLE	WT	ROLE	WT	ROLE	WT
Acoustic-Gravity Waves Nuclear Explosions						

Security Classification

THEORETICAL CALCULATION OF ACOUSTIC-GRAVITY WAVE EXCITATION BY NUCLEAR EXPLOSIONS IN THE ATMOSPHERE

ALEXANDRIA LABORATORIES REPORT NO. AL-72-4

Effective Date of Contract:	1 March 1969
Contract Expiration Date:	31 March 1972
Amount of Contract Dollars:	$ 590,572
Program Code:	1F10
Contract Number:	F-44620-69-C-0082
ARPA Order No.:	1357
Principal Investigator:	Carl A. Newton
Period Covered:	1 March 1969 through 31 March 1972

ic

ABSTRACT

From theoretical calculations of acoustic-gravity waves in the period range 40 to 1,000 seconds from various combinations of yield and burst height, we conclude that the power varies as the square of the yield for low-altitude explosions and as the two-thirds power for altitudes above 100 km. For a given yield, the power increases with burst height to a maximum which is found at lower altitudes for higher yields. The affect of variable atmospheric structure along the propagation paths render it possible to make only a rough estimate of yield and no meaningful estimate of burst height. The study also shows that all of the first ten modes are always relatively well excited so that the relative modal structure of a signal is not a good diagnostic for burst height.

TABLE OF CONTENTS

LIST OF FIGURES

LIST OF FIGURES (Cont'd.)

INTRODUCTION

The continuing tests of nuclear weapons in the atmosphere have prompted interest in using infrasonic data recorded at distant stations to estimate yields and burst heights of the sources. We have calculated theoretical barograms for a variety of yields and burst heights, synthesizing the barograms from the acoustic-gravity wave modes which propagate in the period range of the operating microbarograph arrays, i.e., periods of 4 to 14 minutes. We show examples of barograms recorded at teleseismic distances for many combinations of heights and yields, and draw tentative conclusions about diagnostics which might be deduced from such recordings.

METHOD

The digital computer programs used were those written by Harkrider for calculation of the modal excitation of acoustic-gravity waves (Harkrider, 1964; Harkrider and Flinn, 1970). The original programs used a mass-injection source; we modified these programs to use instead Pierce's energy injection source (Pierce, 1968) which is physically more realistic.

Using these programs it was straightforward to calculate the spectrum and hence the time-domain waveform (via Aki's synthesis technique) for arbitrary yields and burst heights, for any of the various acoustic or gravity modes.

The atmospheric model used was the standard ARDC model (Wares et al., 1960), bounded below by a rigid surface and above by a free surface. The calculated phase velocity dispersion curves for this model are shown in Figure 1.

For standard instrumentation in use, and at an epicentral distance of 10,000 km, only the fundamental gravity mode GR_0 and the lowest acoustic modes S_0 through S_3 are involved in synthesis of waveforms. We calculated theoretical barograms for each of these gravity and acoustic modes, as well as their relative excitation for each yield and source height. The composite barograms in Figures 2 through 10 were constructed from the scaled modal barograms. The notches in the spectra are due to the wave-guide propagation, but we believe that the ripple is probably an artifact

of the synthesis algorithm we employed.

The maxima in the long-period spectra (1 minute) are shown in Figures 11 through 13. The general conclusions we draw from these figures are that: (1) the long-period power varies as the square of the yield for low-altitude explosions, and as the two-thirds power for high altitudes (h>100 km); (2) for a given yield, the long-period power increases with burst height to a maximum, which occurs at lower altitudes for higher yields.

Because of winds and nonuniform atmospheric structure along the signal propagation paths (effects which we have not taken into account in the present work) only a rough estimate of yield can be made from the observational data, and no meaningful estimate of burst height can be attempted.

Acoustic spectrograms from atmospheric explosions contain energy at periods as low as a few seconds. In order to identify the corresponding acoustic-gravity wave modes, we calculated the medium response for all the acoustic modes from S_0 to S_{18}, at periods down to a few seconds. We chose ten modes to include in a synthesis of the broadband waveforms. The ten modes were GR_0 and S_0 through S_8) over the frequency intervals shown in Figure 14. To test the importance of the higher acoustic modes for identifying source height, we calculated theoretical barograms for five source altitudes from 1 km to 45 km. The theoretical barograms for each of ten modes for a source yield of 100 kT at an altitude of 5 km are shown in Figure 15. The moving-window power

spectra for a composite barogram consisting of 5 modes is shown in Figure 16; Figure 17 shows a ten-mode composite.

The composite waveforms for five-mode and ten-mode synthesis are shown in Figures 18 through 20 for yields of 1 kT and 100 kT and altitudes of 1 km, 5 km, and 15 km. It is clear from observational data that attenuation and scattering reduces the higher mode amplitudes much more than the lower mode orders. The high-frequency ripple seen in the ten-mode composites is an artifact introduced by the relatively narrow frequency interval in the synthesis.

The peak overpressures for each of the ten modes are shown in Figure 21. This shows that all ten modes are relatively well excited, and makes it clear that relative modal overpressure is not a good diagnostic for burst height.

REFERENCES

Harkrider, D.G., 1964, Theoretical and observed acoustic-gravity waves from explosive sources in the atmosphere: J. Geophys. Res., v. 69, p. 5295-5321.

Harkrider, D.G. and Flinn, E.A., 1970, Effect of crustal structure on Rayleigh waves generated by atmospheric explosions: Revs. Geophys., Space Phys., v. 8, p. 501-516.

Pierce, A.D., 1968, Theoretical source models for the generation of acoustic-gravity waves by nuclear explosions, in acoustic-gravity waves in the atmosphere: ed. T.M. Georges, Environmental Science Services Administration, U.S. Department of Commerce, Boulder, Colorado.

Wares, G.W., Champion, K.W., Pond, H.L., and Cole, A.E., 1960, Model atmospheres, in Handbook of Geophysics, 1-1-1-37, The Macmillan Company, New York.

ACKNOWLEDGEMENT

This research was sponsored by the Air Force Office of Scientific Research under Contract No. F-14620-69-C-0082.

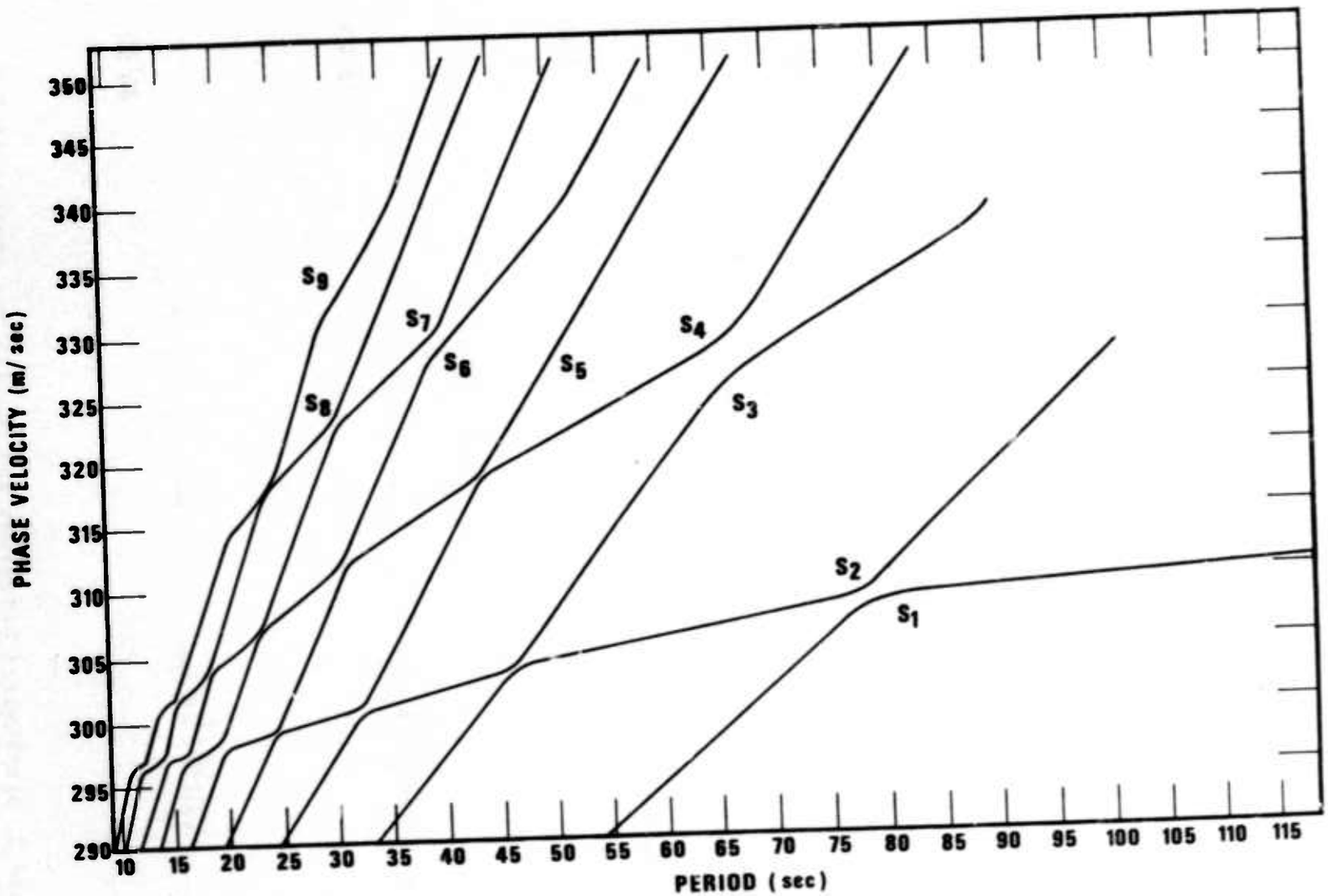

Figure 1. Dispersion curves for acoustic-gravity wave modes in the period range 6 - 115 seconds. GR_0 is the fundamental gravity mode; the acoustic modes are labelled "S", with the subscript indicating the mode order.

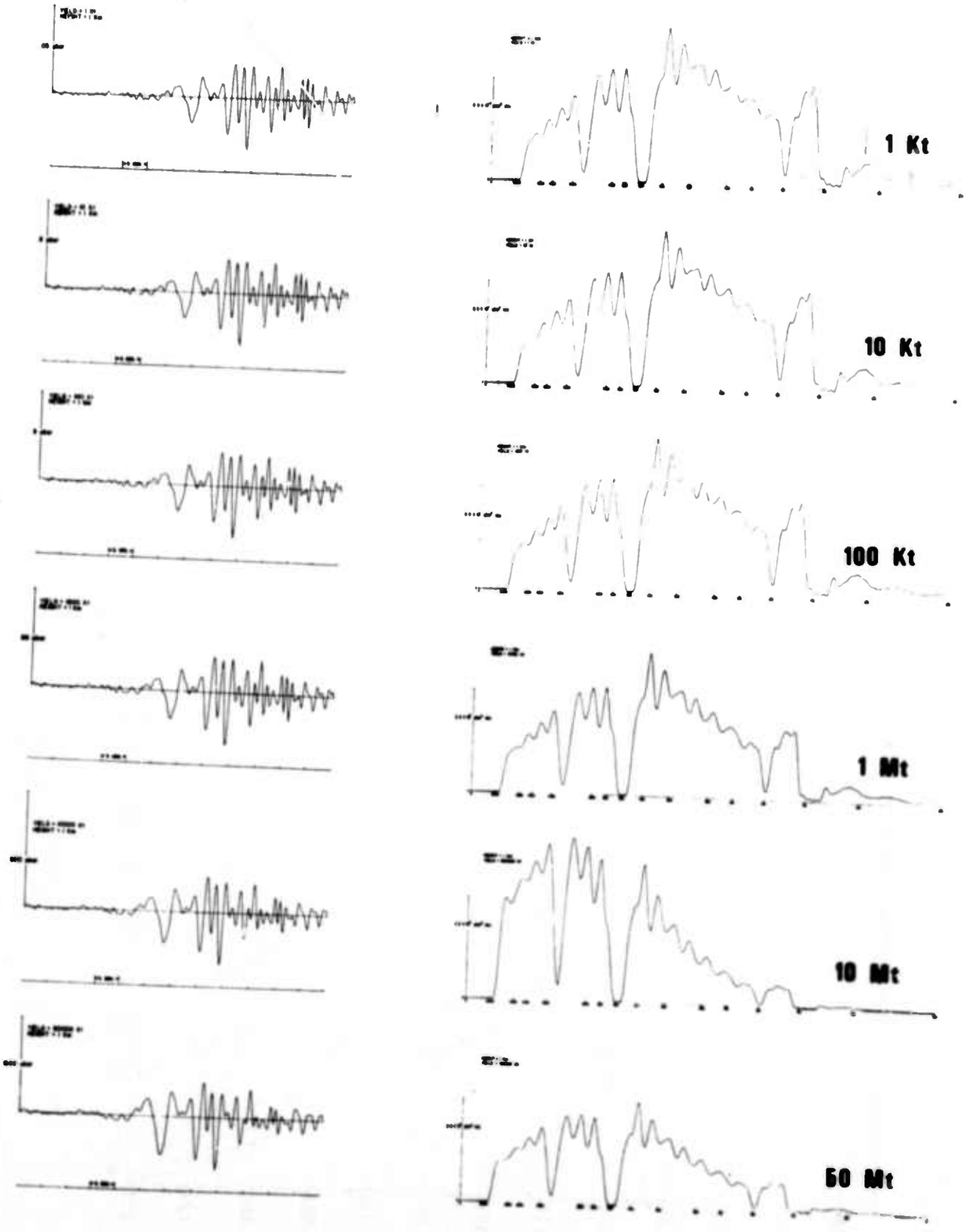

Figure 2. Synthesized barograms and spectra for sources at 1 km altitude and yields from 1 kT to 50 MT. Each record extends over the group velocities from 333 to 290 m/s, beginning 400 minutes after an event 8000 km distant. The horizontal axes are scaled in seconds of period.

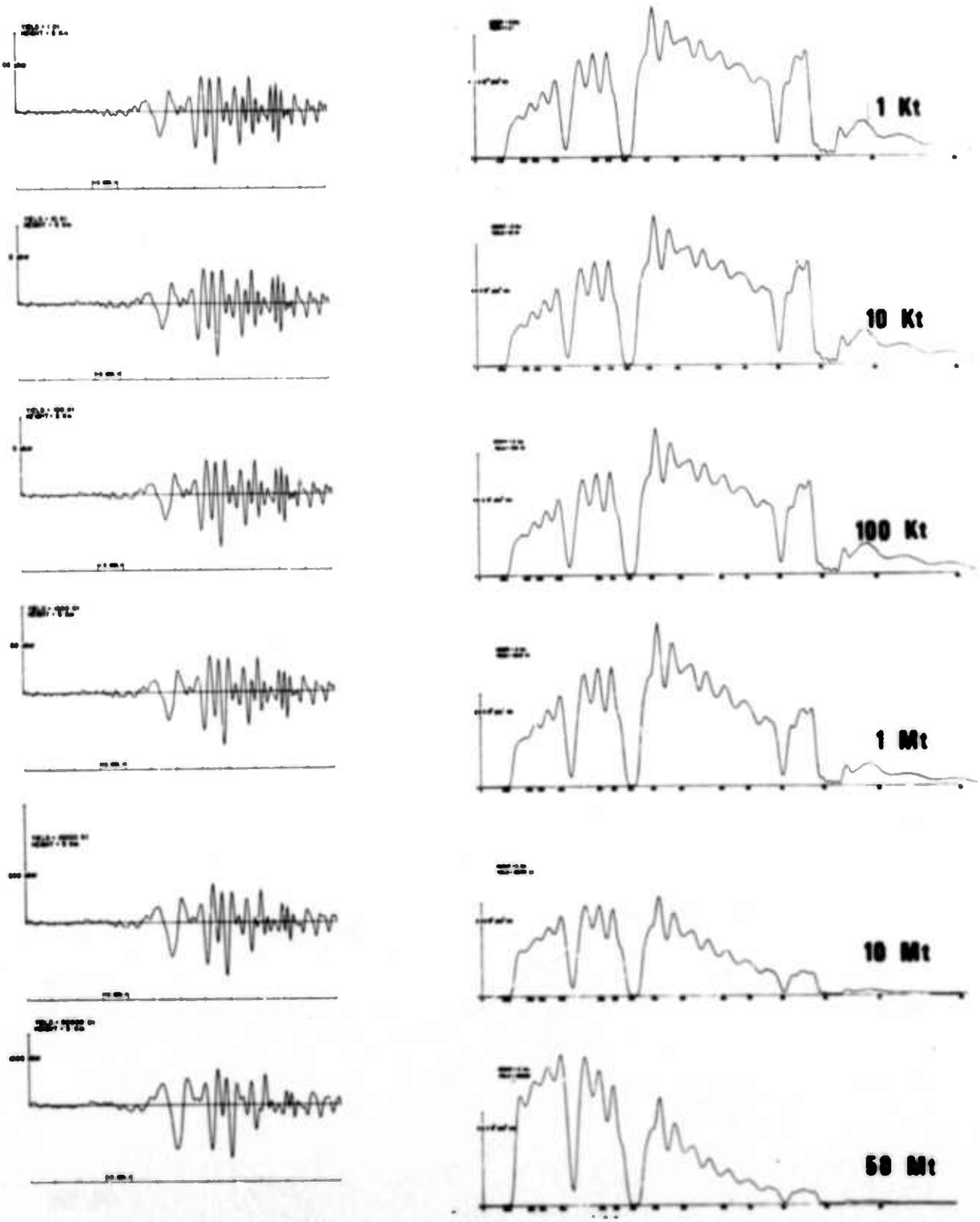

Figure 3. Synthesized barograms and spectra for sources at 5 km altitude and yields from 1 kT to 50 MT. Each record extends over the group velocities from 333 to 290 m/s, beginning 400 minutes after an event 8000 km distant. The horizontal axes are scaled in seconds of period.

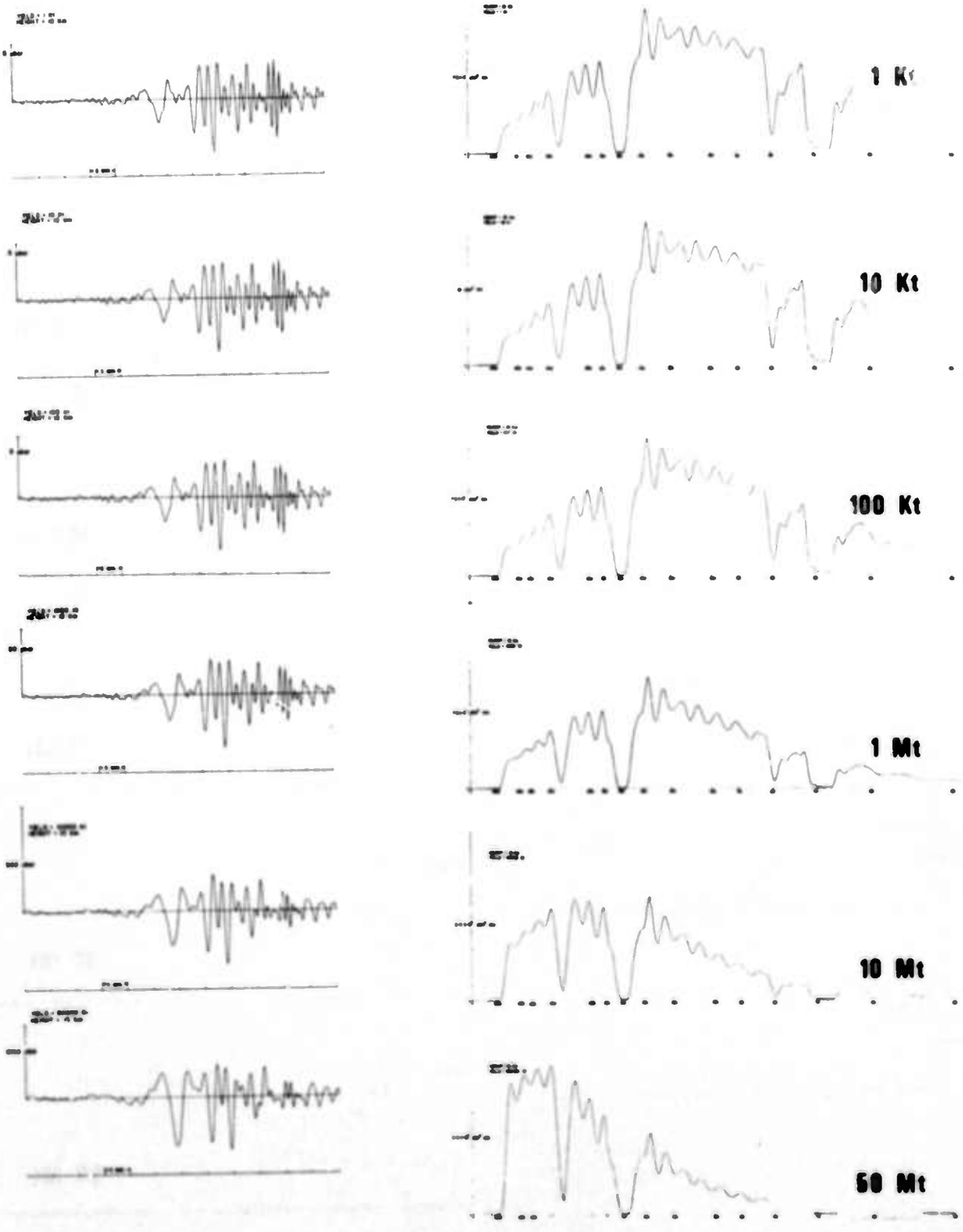

Figure 4. Synthesized barograms and spectra for sources at 10 km altitude and yields from 1 kT to 50 MT. Each record extends over the group velocities from 333 to 290 m/s, beginning 400 meters after an event 8000 km distant. The horizontal axes are scaled in seconds of period.

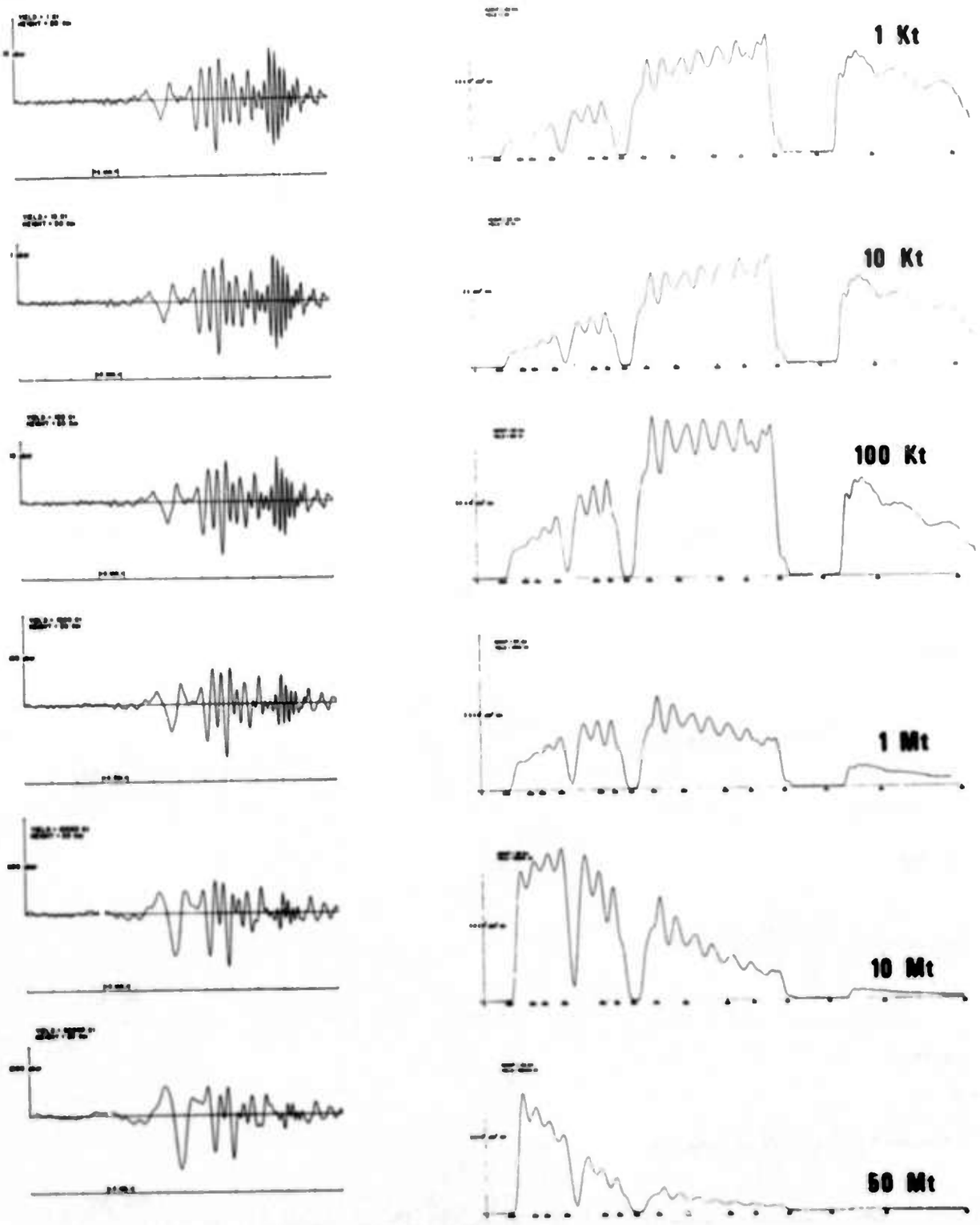

Figure 5. Synthesized barograms and spectra for sources at 20 km altitude and yields from 1 kT to 50 MT. Each record extends over the group velocities from 333 to 290 m/s, beginning 400 minutes after an event 8000 km distant. The horizontal axes are scaled in seconds of period.

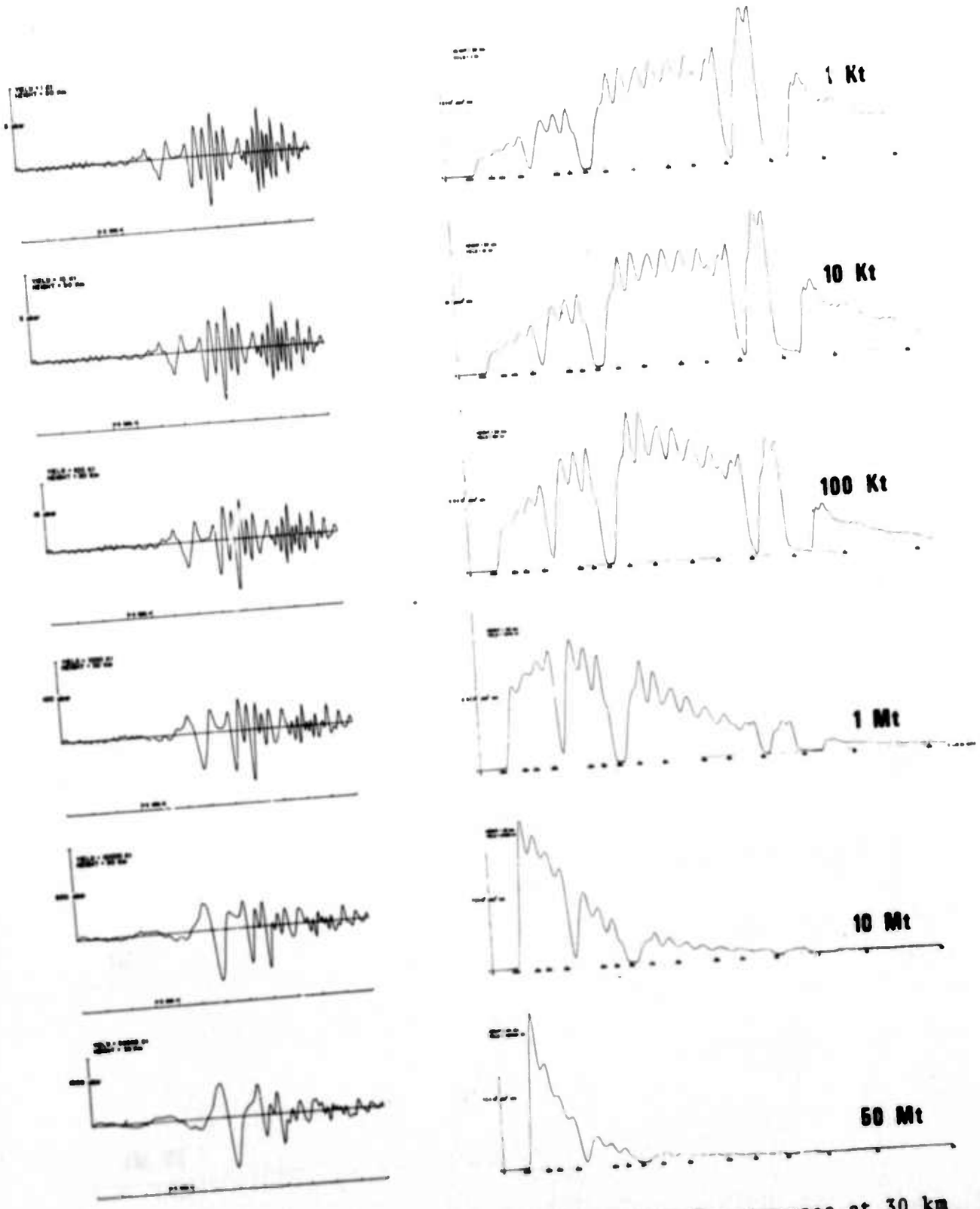

Figure 6. Synthesized barograms and spectra for sources at 30 km altitude and yields from 1 kT to 50 MT. Each record extends over the group velocities from 333 to 290 m/s, beginning 400 minutes after an event 8000 km distant. The horizontal axes are scaled in seconds of period.

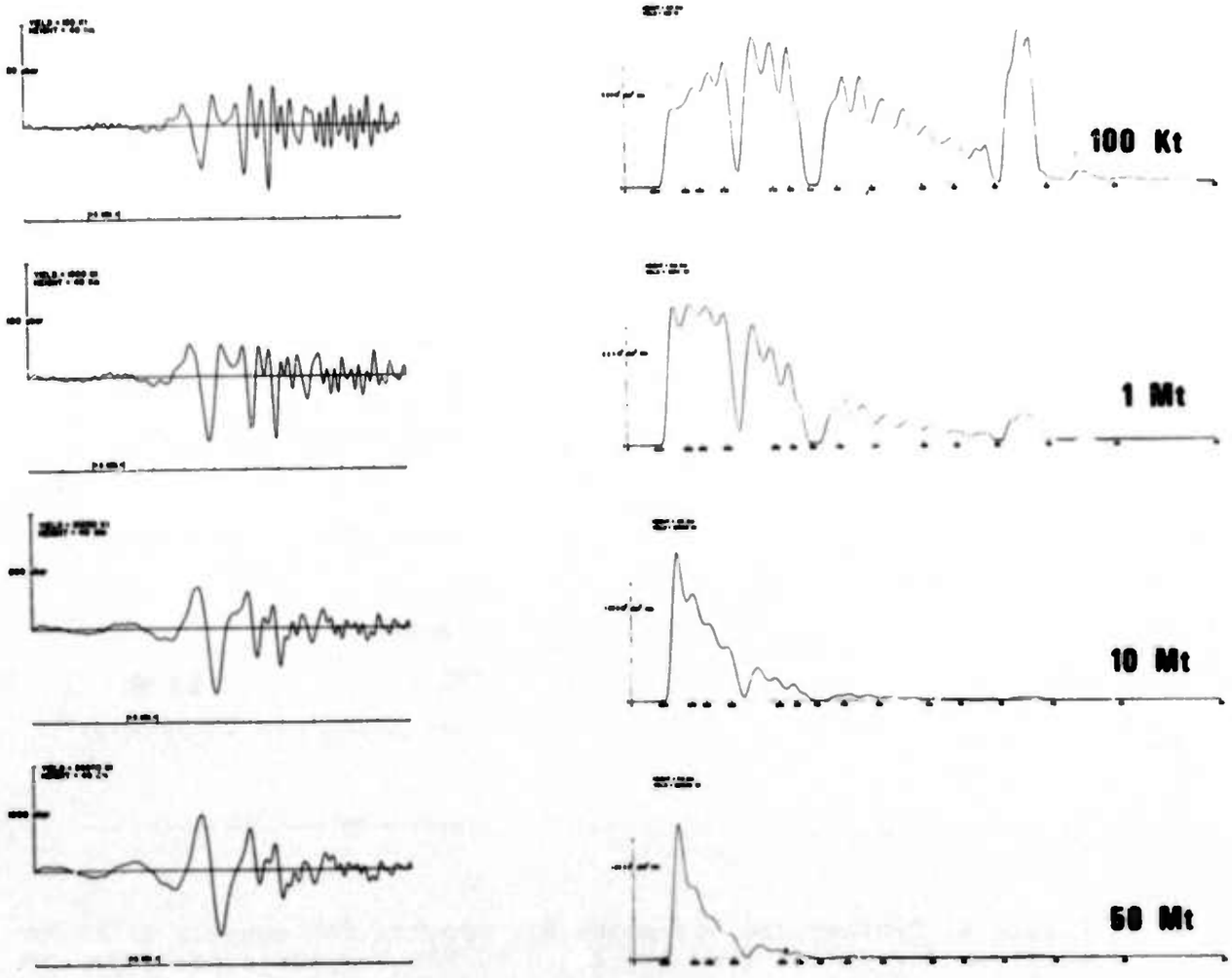

Figure 7. Synthesized barograms and spectra for sources at 40 km altitude and yields from 100 kT to 50 MT. Each record extends over the group velocities from 333 to 290 m/s, beginning 400 minutes after an event 8000 km distant. The horizontal axes are scaled in seconds of period.

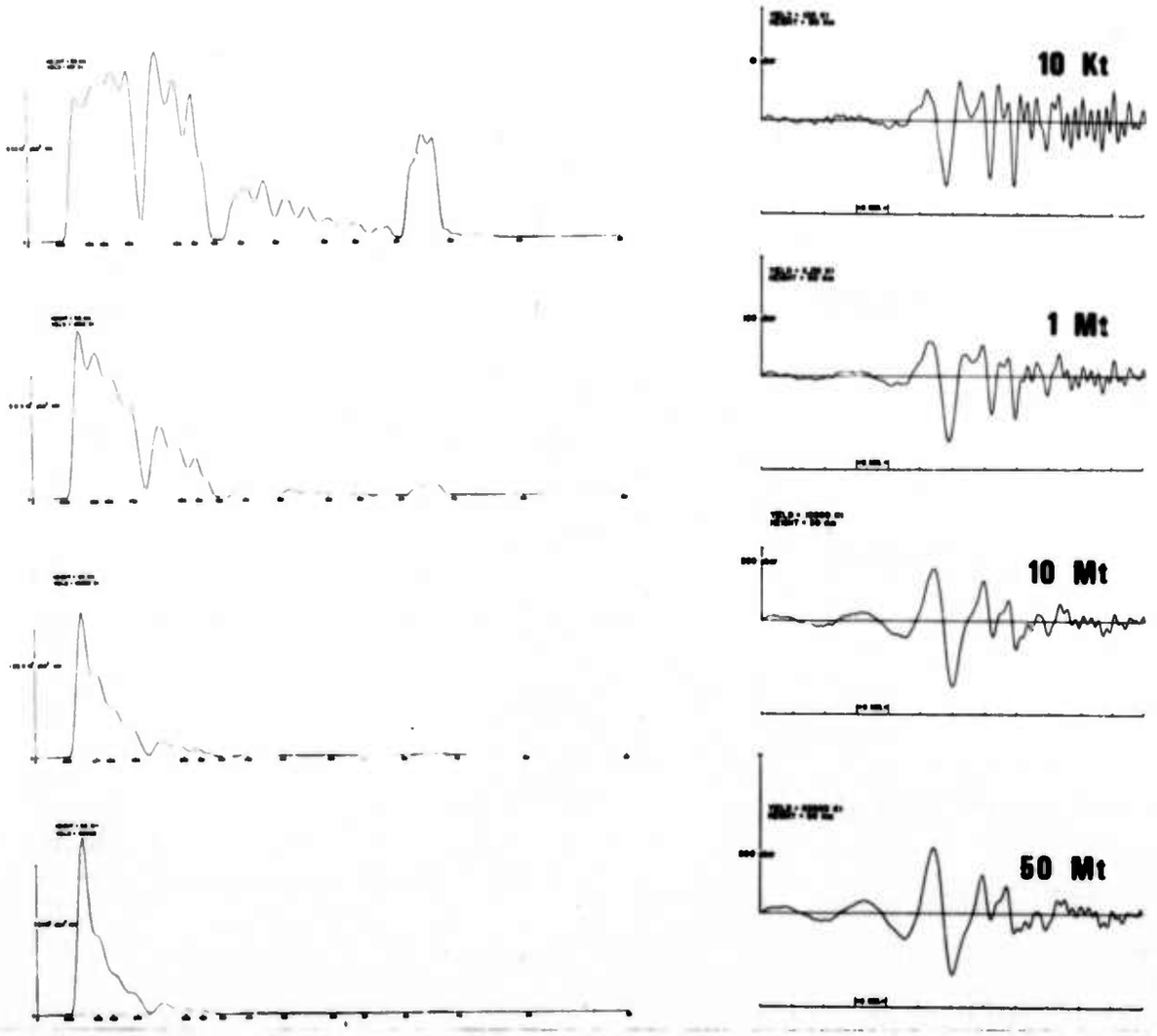

Figure 8. Synthesized barograms and spectra for sources at 50 km altitude for yields from 100 kT to 50 MT. The horizontal axes are scaled in seconds of period. Each record extends over the group velocities from 333 to 290 m/s, beginning 400 minutes after an event 8000 km distant.

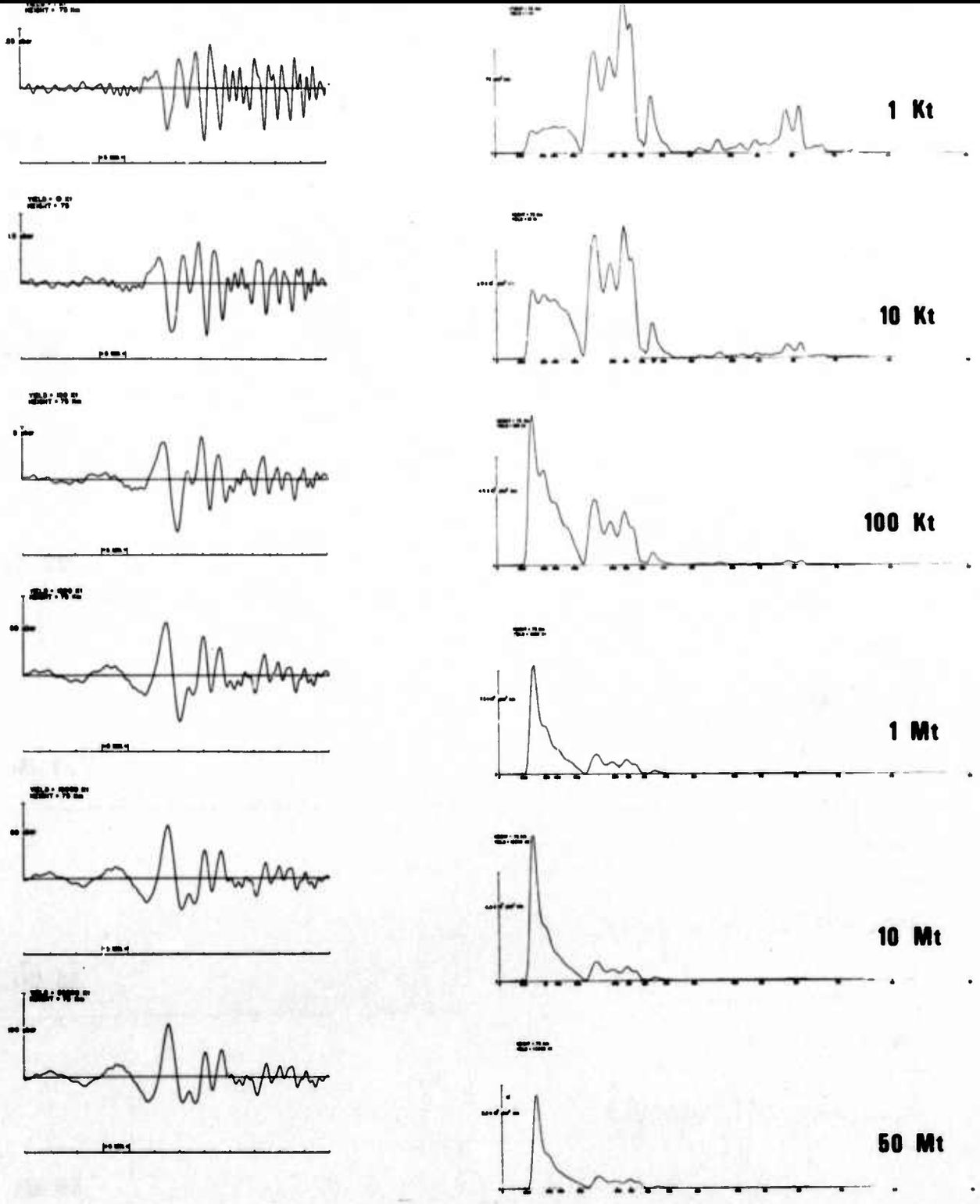

Figure 9. Synthesized barograms and spectra for sources at 75 km altitude and yields from 1 kT to 50 MT. Each record extends over the group velocities from 333 to 290 m/s, beginning 400 minutes after an event 8000 km distant. The horizontal axes are scaled in seconds of period.

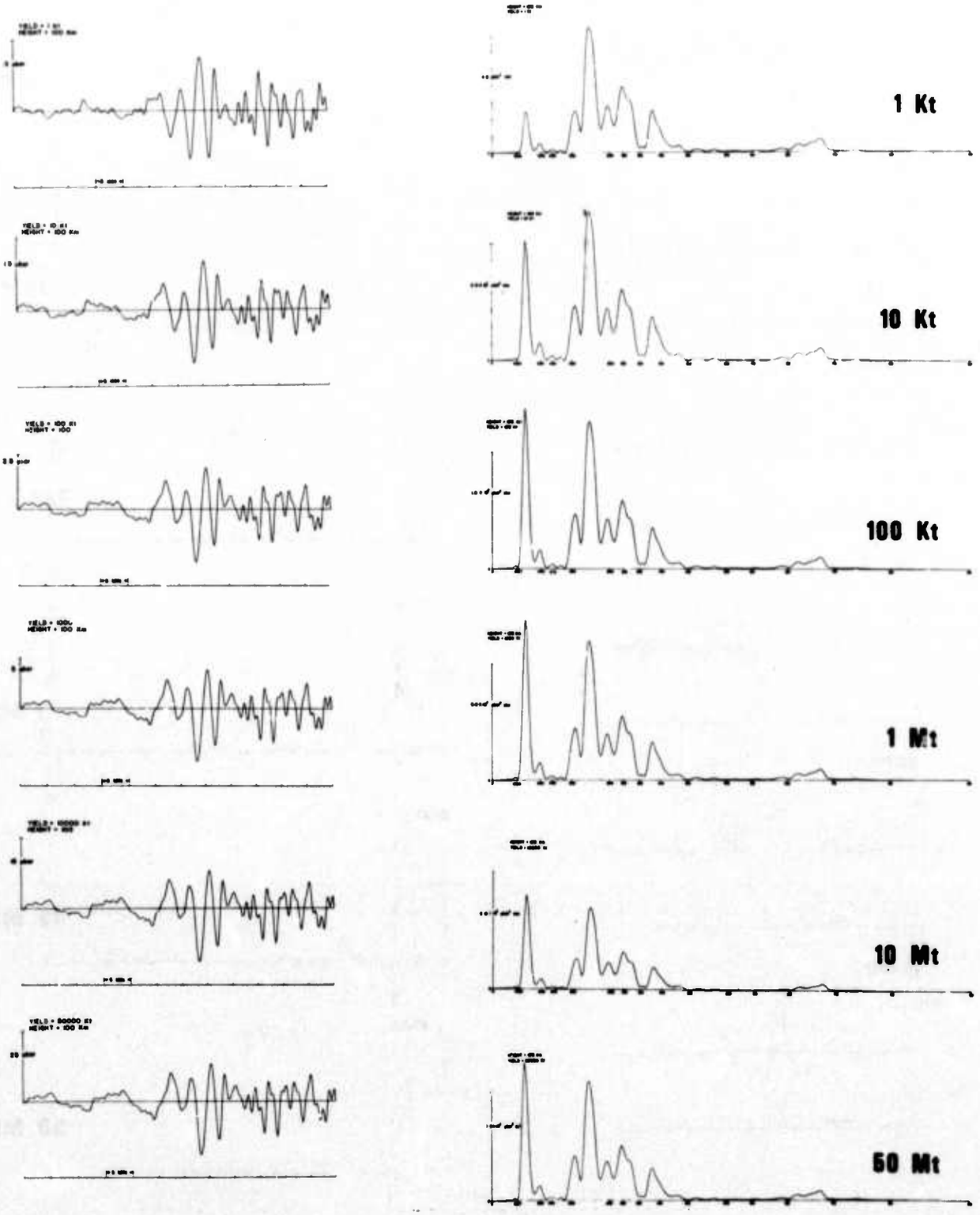

Figure 10. Synthesized barograms and spectra for sources at 100 km altitude for yields from 1 kT to 50 MT. Each record extends over the group velocities from 333 to 290 m/s, beginning 400 minutes after an event 8000 km distant. The horizontal axes are scaled in seconds of period.

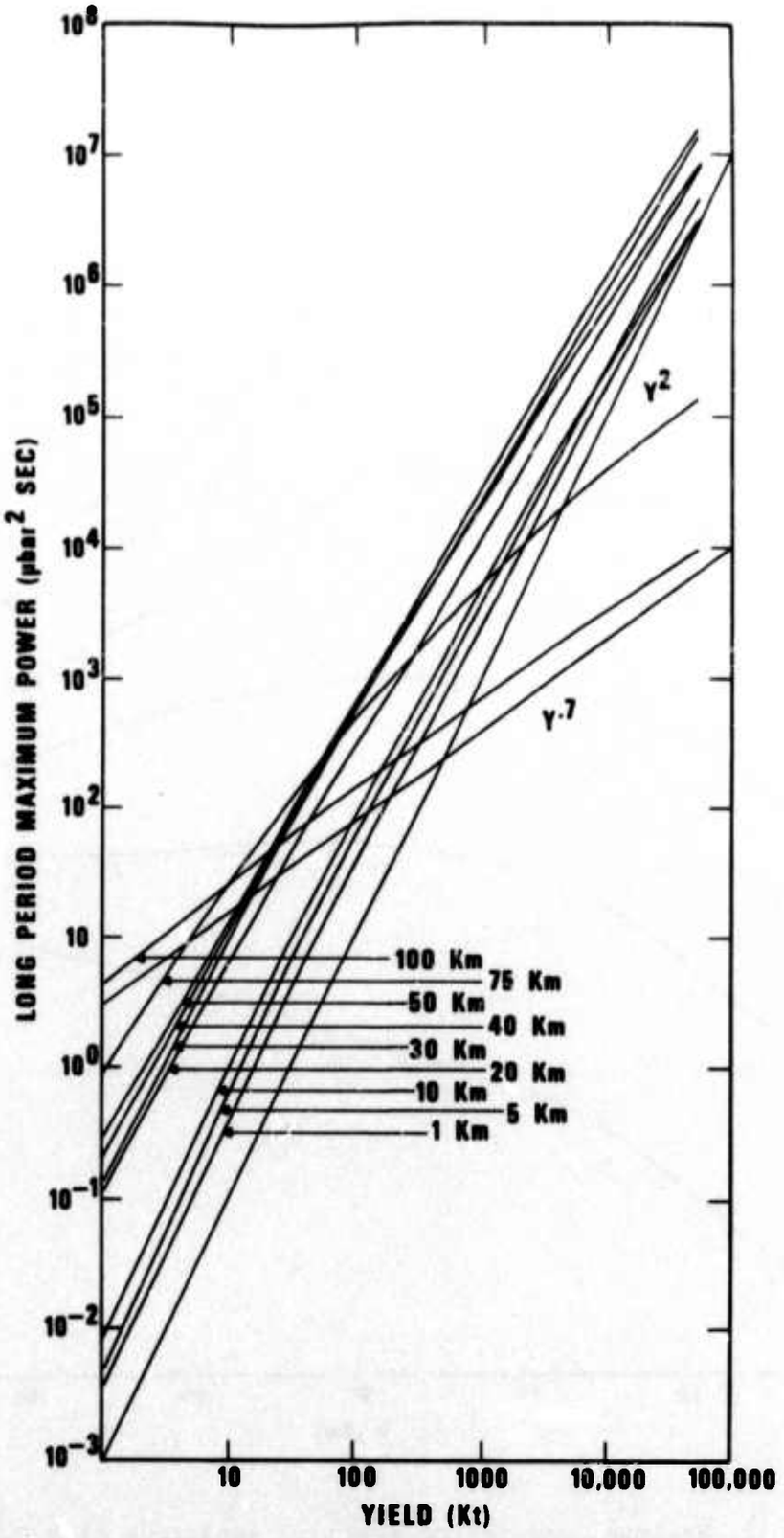

Figure 11. Variation of long-period maximum amplitude (taken for periods greater than one minute) with yield and burst height.

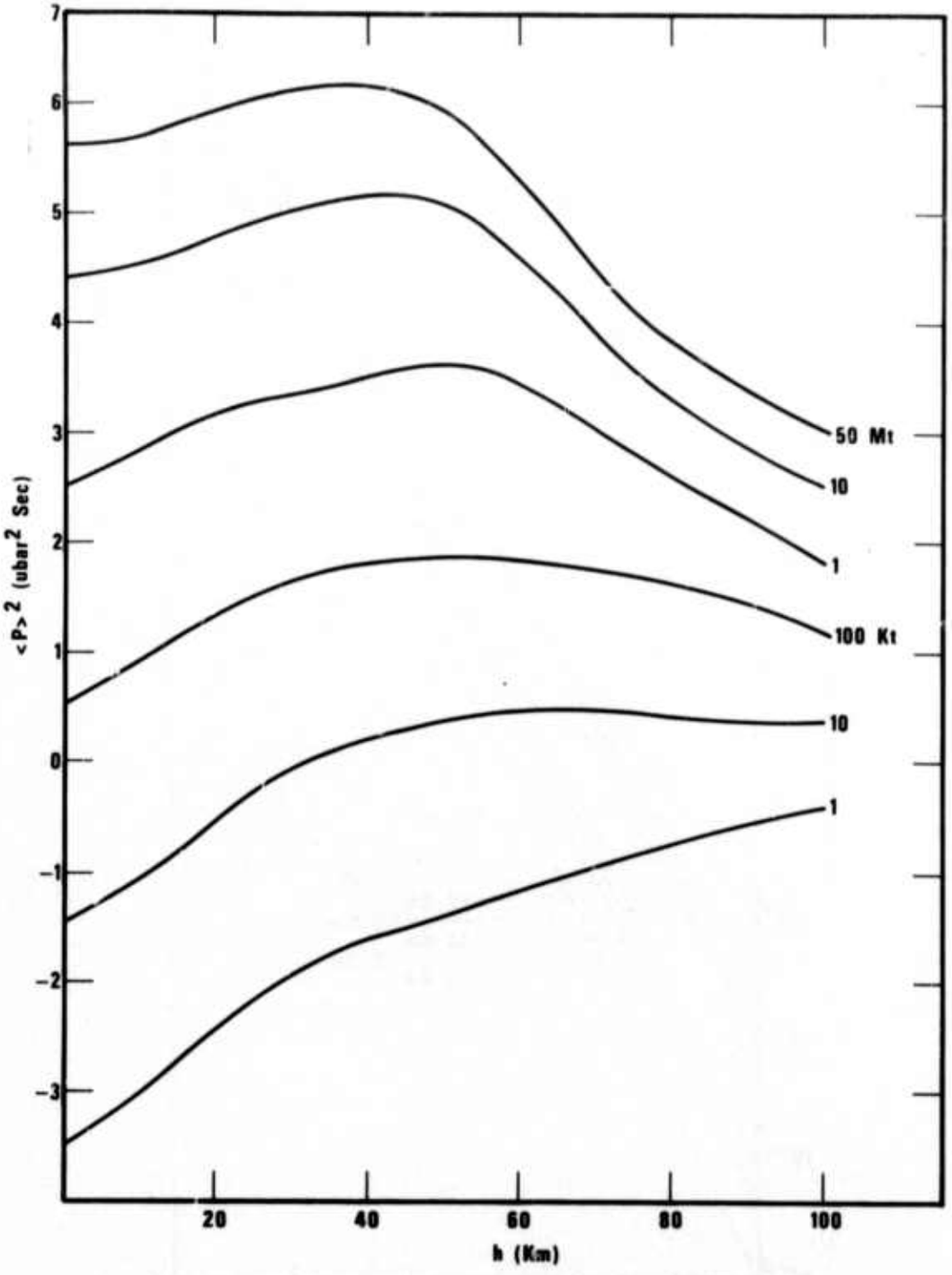

Figure 12. Maximum long-period spectral amplitude as a function of burst height.

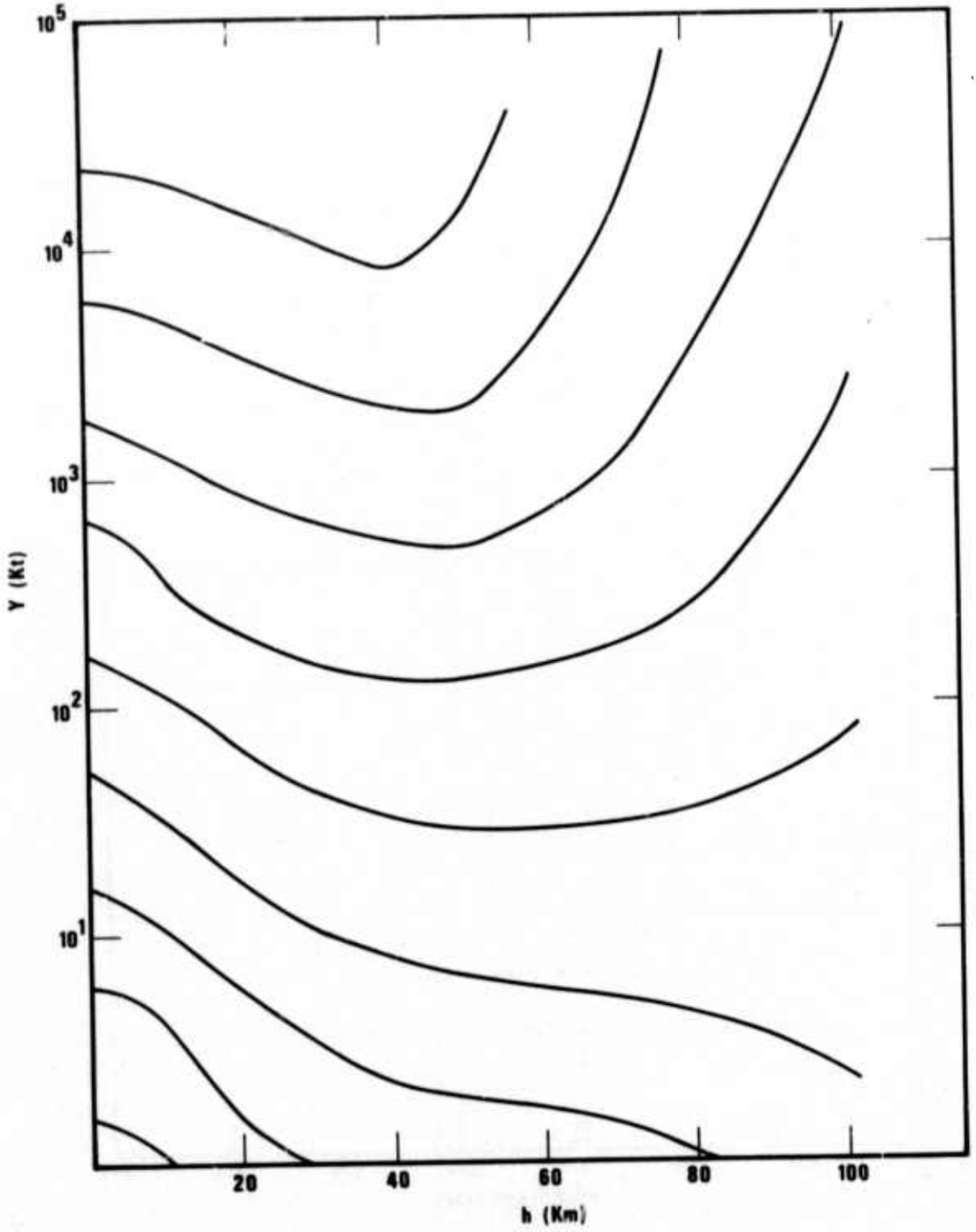

Figure 13. Maximum long-period spectral amplitude contoured as a function of both yield and burst height.

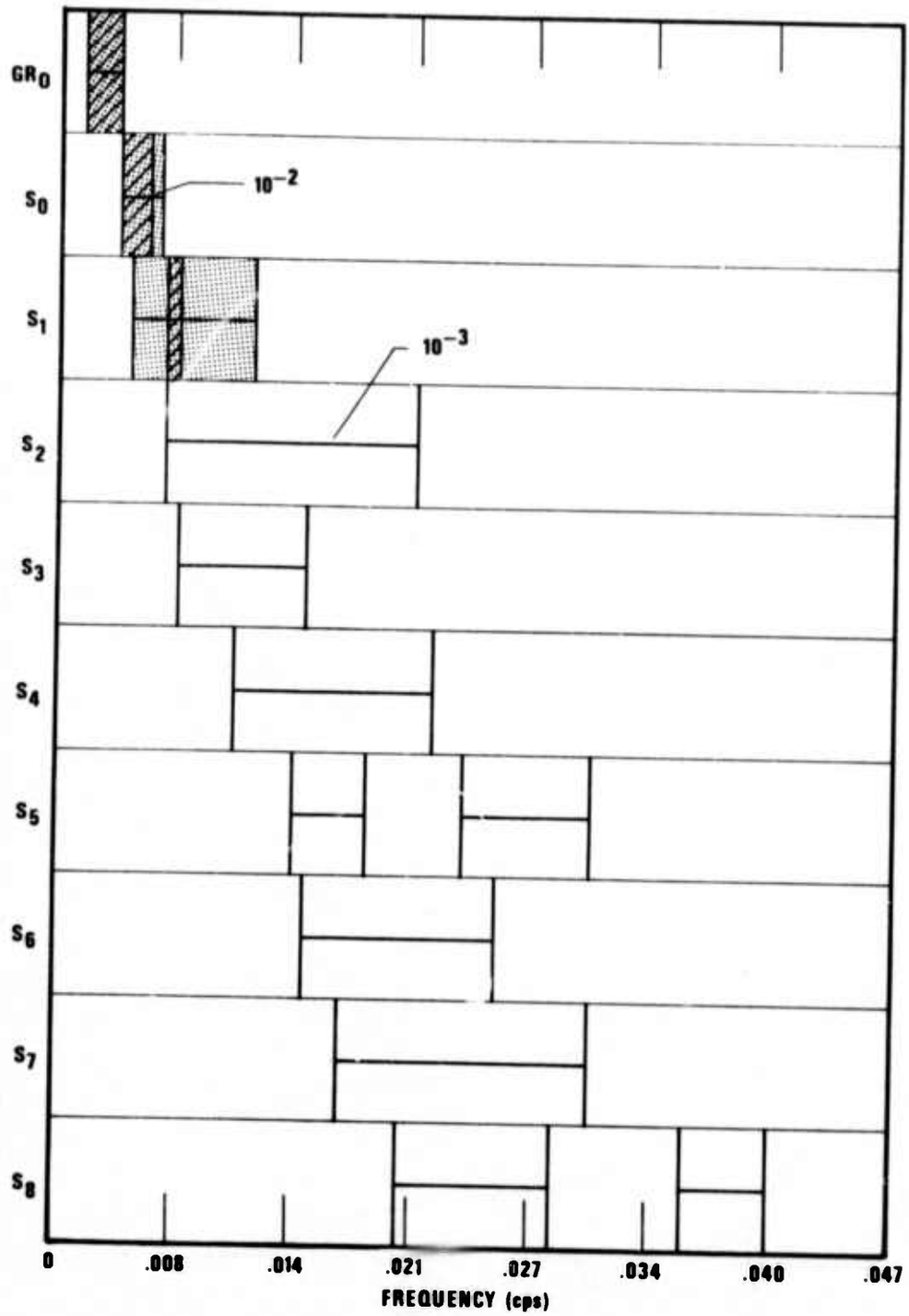

Figure 14. Excitation of acoustic-gravity modes for a unit source amplitude. The hatchured regions show the frequencies where modal excitation is greater than 10^{-2}, and the bars indicate excitation greater than 10^{-3}.

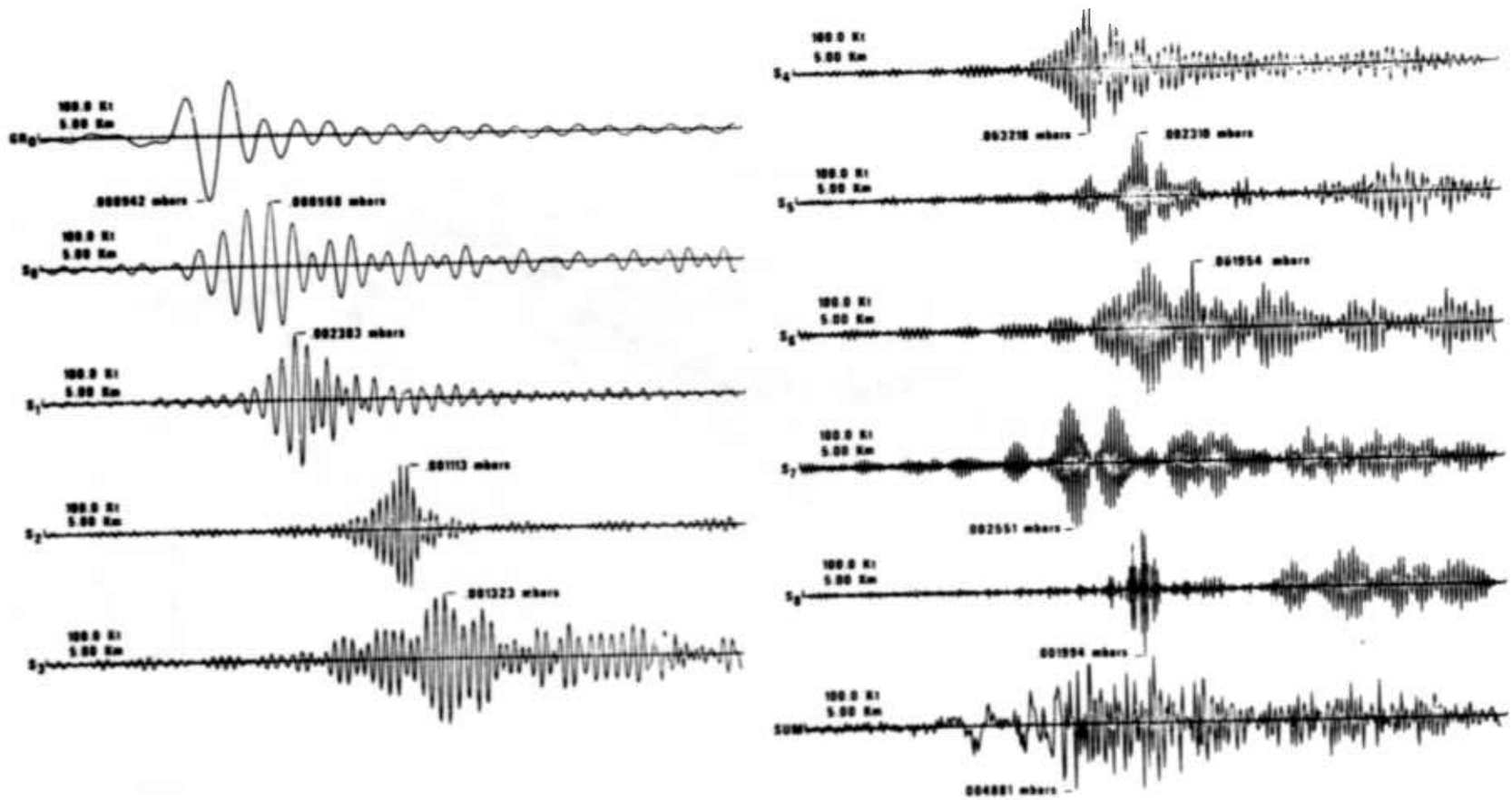

Figure 15. Individual modal excitation for a 100 kT explosion at 5 km altitude. (a) GR_0; (b) through (j) S_0 through S_8; (k) (k) composite barogram. The last figure in the label of each trace indicates the maximum trace amplitude in microbars.

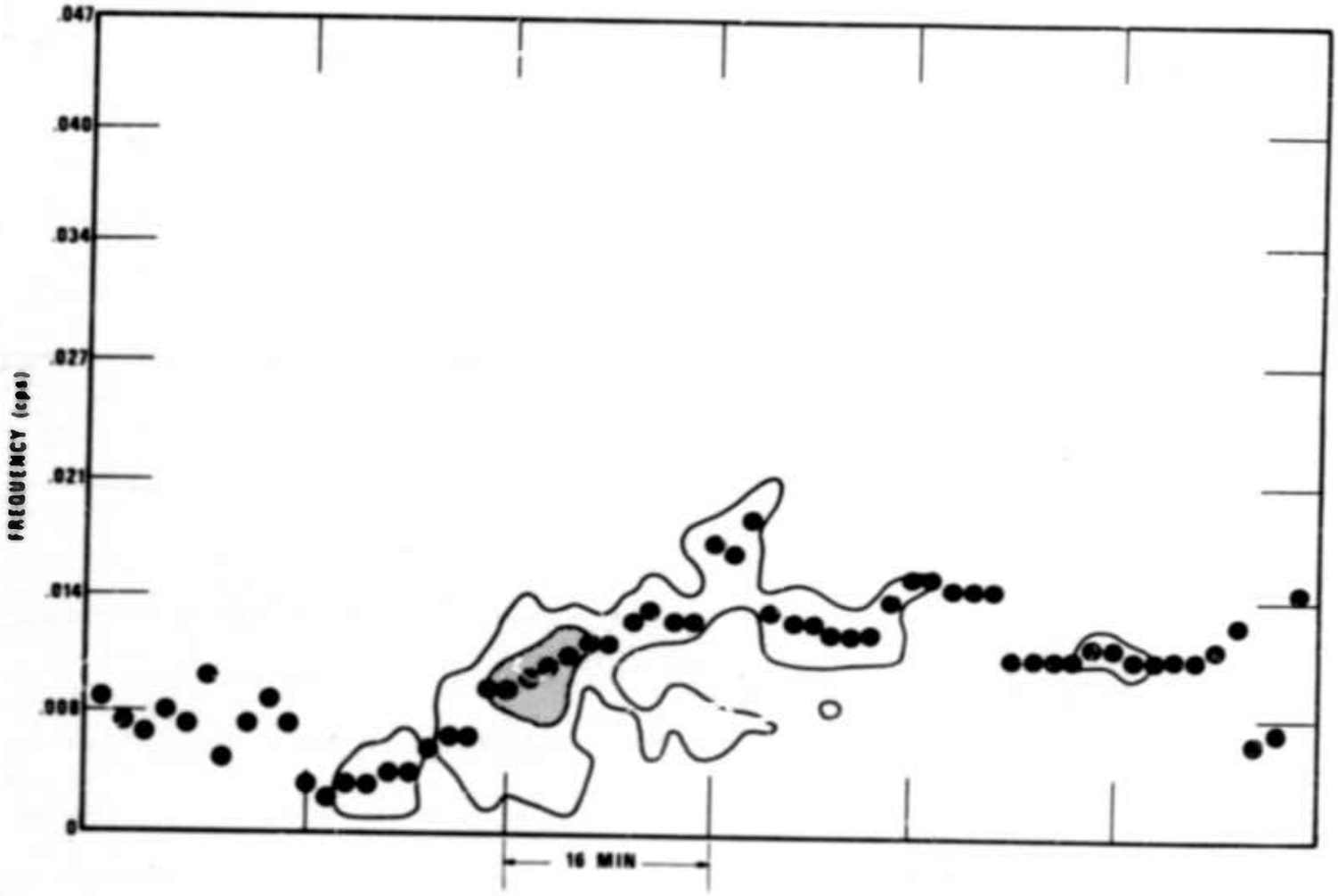

Figure 16. Time-varying spectrogram for the synthetic barogram from a 100 kT source at 5 km altitude, with five modes.

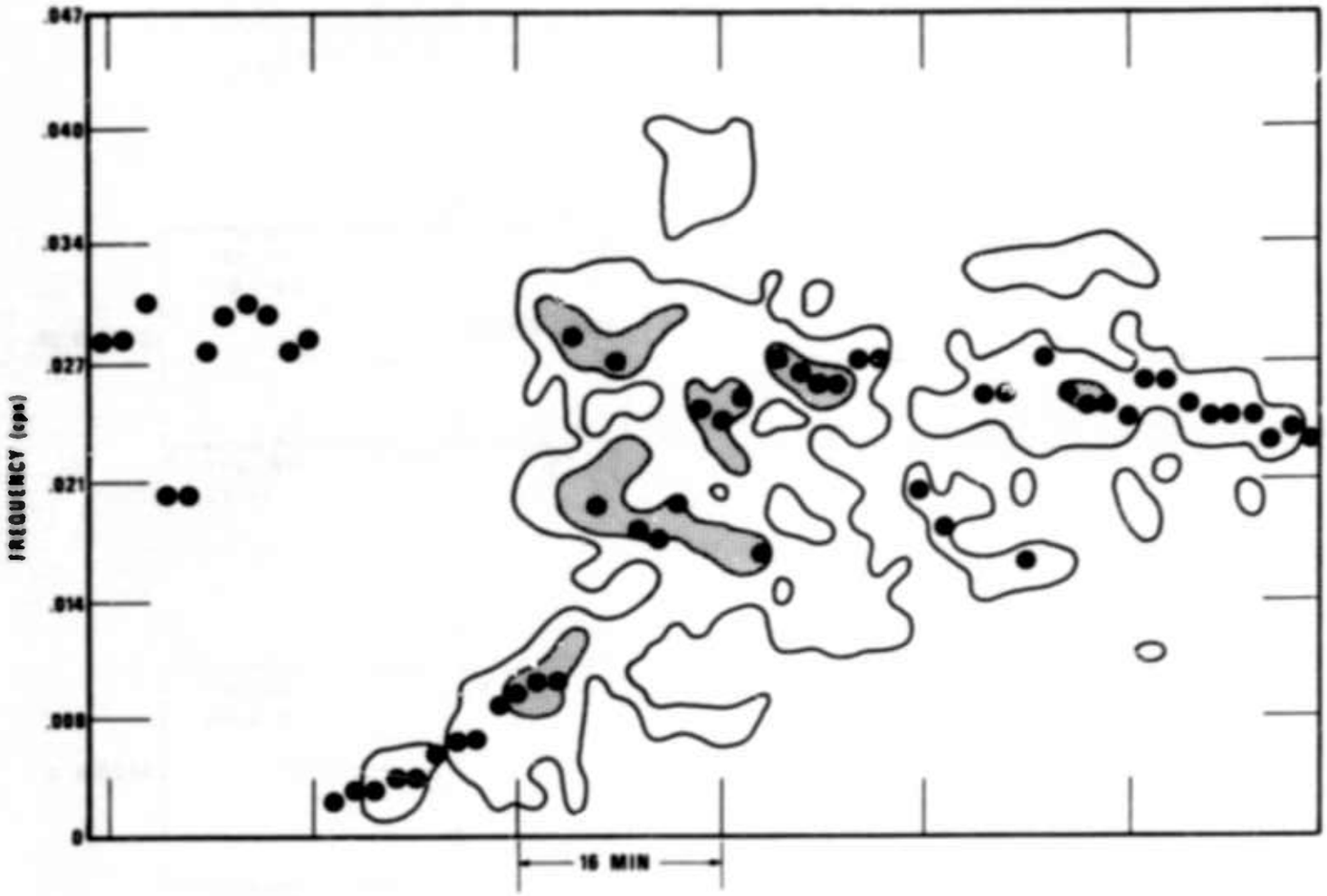

Figure 17. Time-varying spectrogram for the synthetic barogram from a 100 kT source at 5 km altitude, with ten modes.

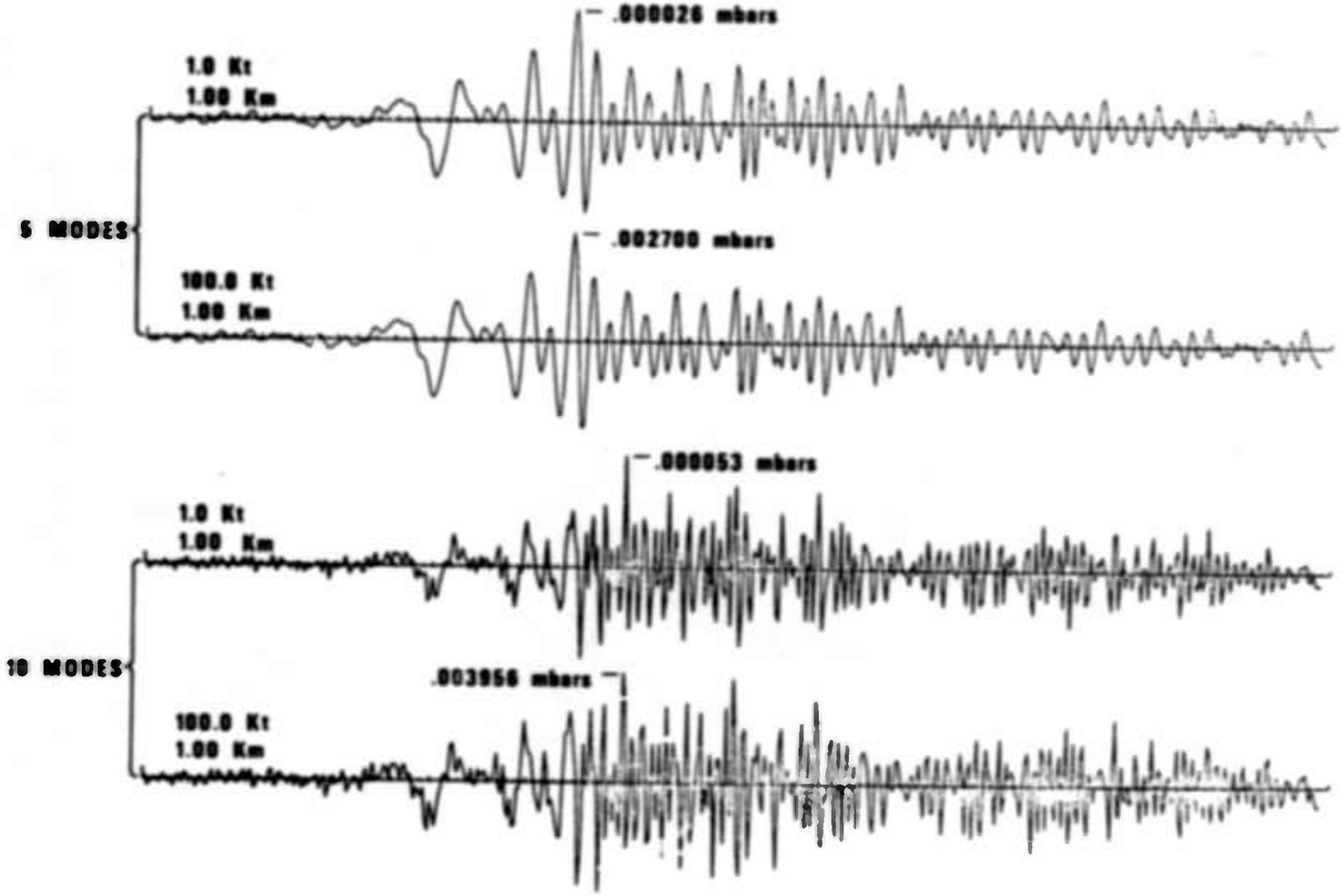

Figure 18. Composite synthesized barograms for yields of 1 kT and 100 kT at an altitude of 1 km. The upper two curves are the synthesis for five modes; the lower two for synthesis of ten modes.

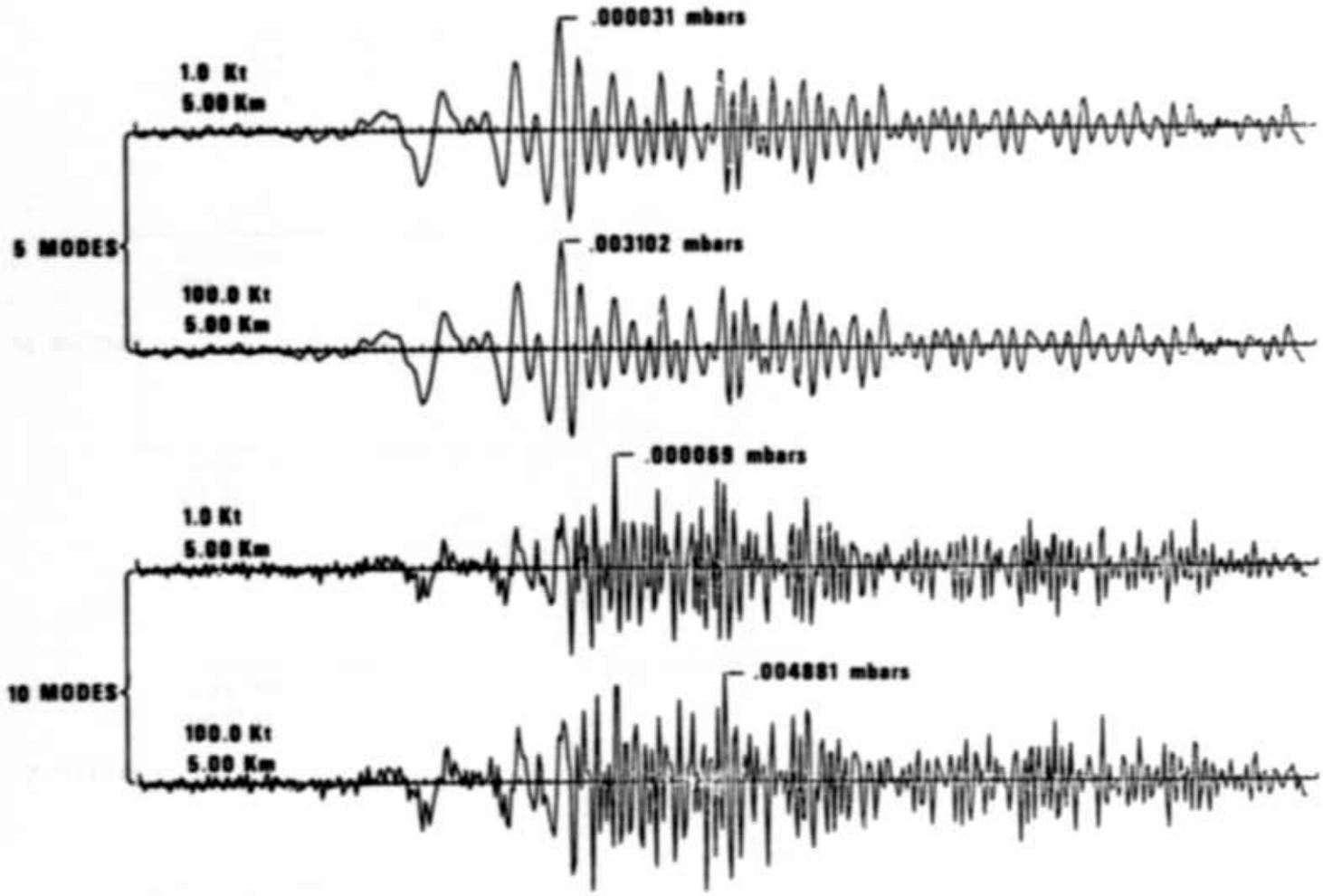

Figure 19. Composite synthetic barograms for yields of 1 kT and 100 kT at an altitude of 5 km. The upper two curves are the synthesis for five modes; the lower two for synthesis of ten modes.

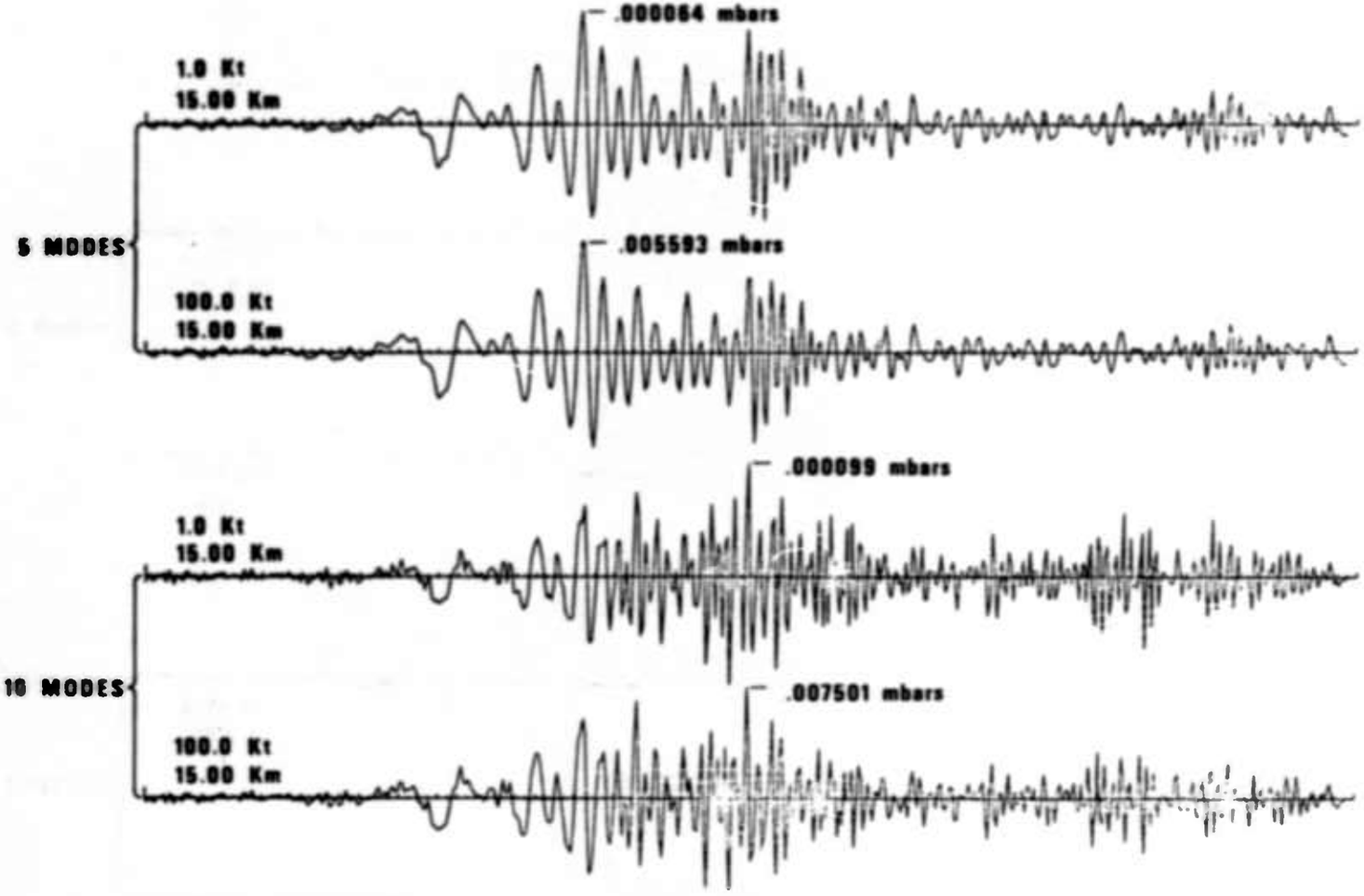

Figure 20. Composite synthetic barograms for yields of 1 kT and 100 kT at an altitude of 15 km. The upper two curves are the synthesis for five modes; the lower two for synthesis of ten modes.

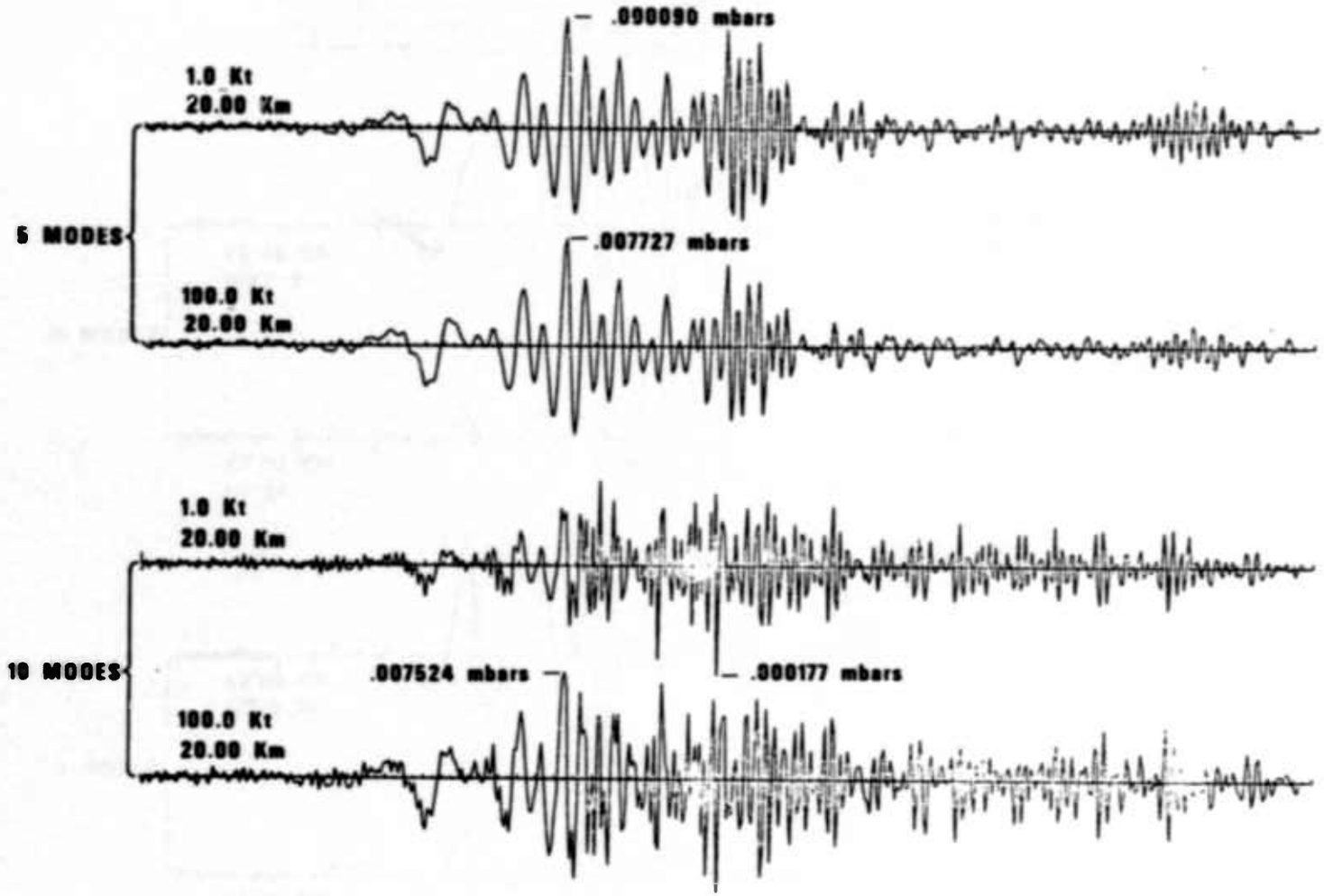

Figure 21. Composite synthetic barograms for yields of 1 kT and 100 kT at an altitude of 20 km. The upper two curves are the synthesis for five modes; the lower two for synthesis of ten modes.

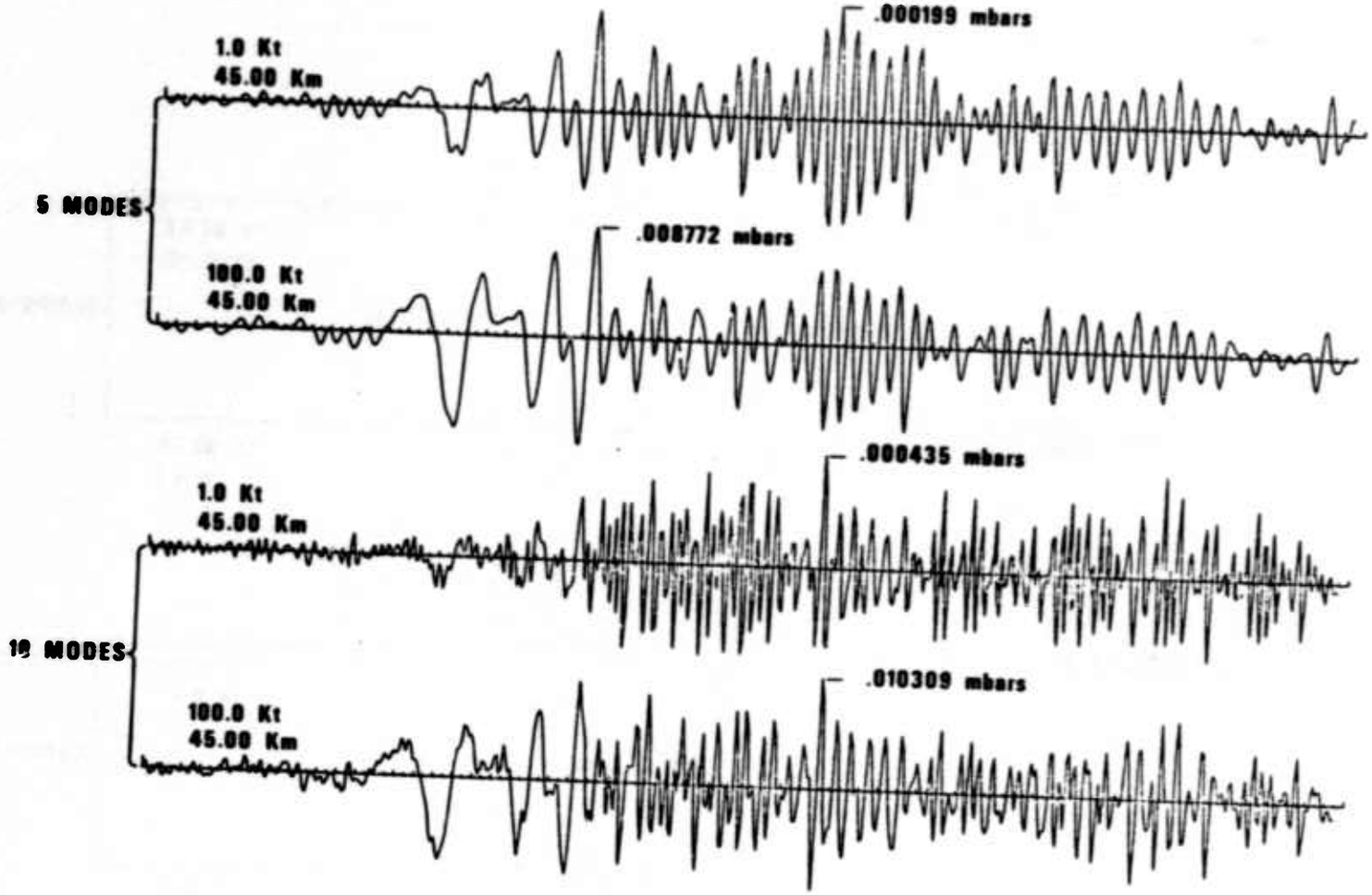

Figure 22. Composite synthetic barograms for yields of 1 kT and 100 kT at an altitude of 45 km. The upper two curves are the synthesis for five modes; the lower two for synthesis of ten modes.

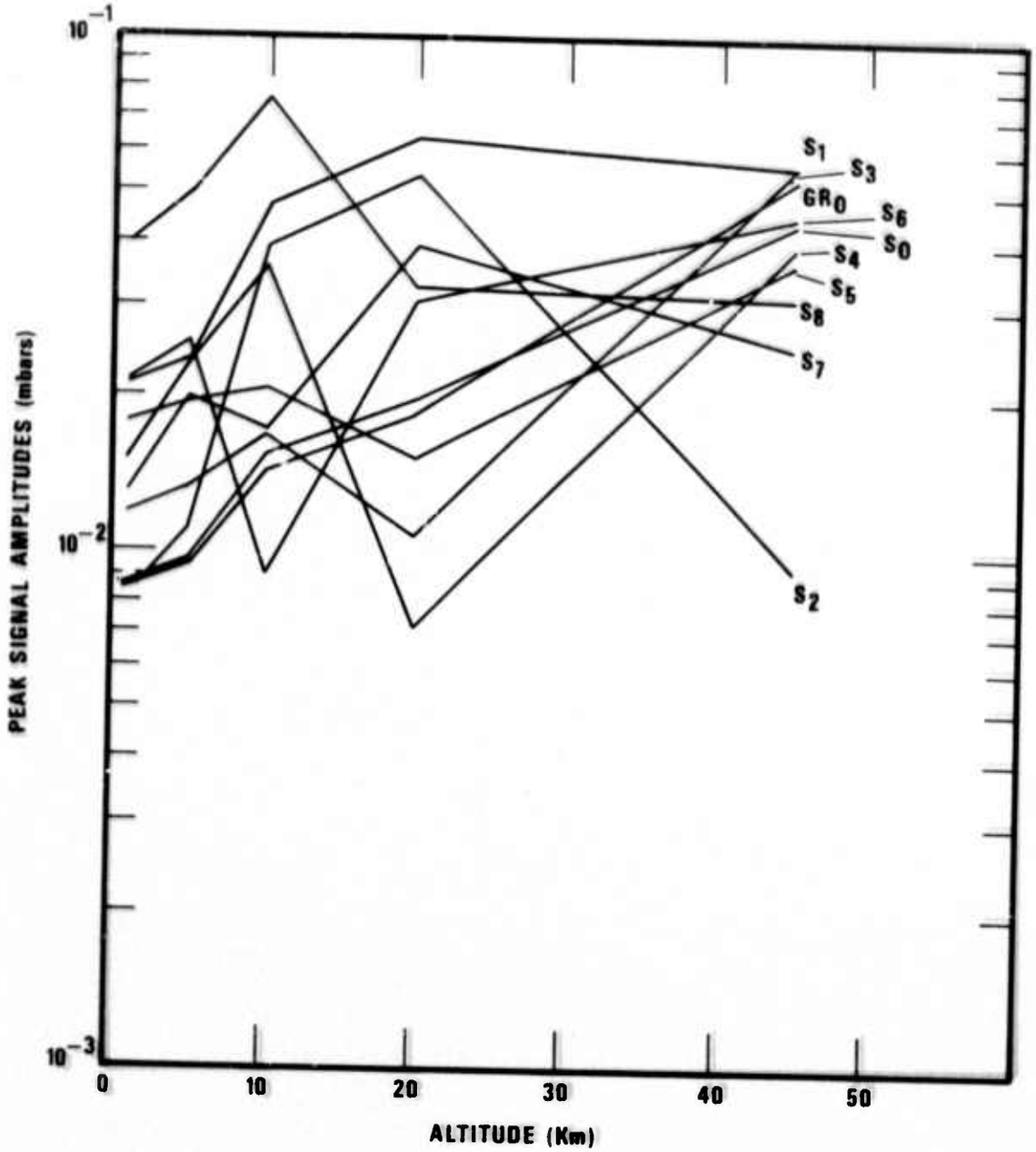

Figure 23. Variation of peak amplitude with altitude for the individual modes used in the barogram synthesis.